

Lung Cancer Prediction using Computed Tomography (CT) Scans with Deep Learning-based Approach

Valluri Gayathri¹, Dr .Yalamanchili Anjani²

M.Tech student, Sir C R Reddy College of Engineering, Eluru, India

Associate Professor, Department of CSE, Sir C R Reddy College of Engineering, Eluru, India

ABSTRACT: This research presents an automatic lung cancer classification and prediction system using computed tomography (CT) scans, leveraging Deep Learning (DL) strategies with Enhanced Convolutional Neural Networks (CNNs) for rapid and accurate image analysis. Pre-trained models, including ConvNeXtSmall, VGG16, ResNet50, InceptionV3, and EfficientNetB0, were developed and evaluated for lung cancer classification. The dataset comprised four classes: adenocarcinoma (338 images), large cell carcinoma (187 images), squamous cell carcinoma (260 images), and normal (215 images). The Enhanced CNN model achieved a remarkable testing accuracy of 99.09%, surpassing other models, including ConvNeXt (87%), VGG16 (99%), ResNet50 (94.5%), InceptionV3 (76.9%), and EfficientNetB0 (97.9%). Notably, the study reports the first instance of an Enhanced CNN achieving 100% accuracy in testing, marking a significant advancement in lung cancer diagnostics. These findings emphasize the transformative potential of Enhanced CNN models in clinical applications, underscoring the importance of incorporating advanced image enhancement techniques and innovative model architectures for early and precise lung cancer detection.

KEYWORDS: Enhanced Convolutional Neural Networks (CNNs), Lung Cancer (LC), Deep Learning (DL), Computed Tomography (CT)

I. INTRODUCTION

In recent years, artificial intelligence (AI) has gained significant traction in discovering complex relationships between inputs and outputs using dynamic resistance signals, eliminating the need for traditional mathematical models that rely on prior assumptions [1]. Modern AI systems excel at capturing interaction effects and nonlinear relationships [2], which has led to their expansion into various domains that were previously exclusive to human expertise. These include clinical decision-making, predictive medicine, patient data analysis, and health services management [3,4].

AI's growing role in medicine is particularly evident in medical image analysis for diagnostic and predictive applications [5]. Radiologists traditionally interpret medical images, requiring both high-quality imaging and expert interpretation skills. However, challenges such as noise, fatigue, and interpretation bias can affect diagnostic accuracy. AI-powered systems address these issues using advanced imaging and computational methods. AI is now widely applied in tasks like risk evaluation, prognosis, diagnosis, disease detection, and treatment response assessment [6,7]. Machine learning (ML) and deep learning (DL) are the primary drivers behind these advancements. Machine learning algorithms make predictions based on prior data, identifying patterns and meaningful representations from input data [8-10]. Deep learning, a specialized subset of ML, utilizes multiple layers of computational units to analyze data, making it particularly effective for medical image analysis [8,11]. Since the 1960s, machine learning algorithms have been applied to medical imaging, evolving into computer-aided detection/diagnosis (CAD) systems to improve diagnostic accuracy and efficiency [12-14].

Cancer, characterized by uncontrolled cell growth and proliferation, remains one of the leading causes of death worldwide [15]. The human body contains over 30 trillion cells [16], and the natural process of cell division is regulated through programmed cell death. However, when this regulation fails, abnormal cells continue to divide, forming malignant tumors [17-18]. Malignant tumors, unlike benign ones, invade surrounding tissues and spread to distant body regions [19-21]. Lung cancer, in particular, is a major contributor to cancer-related mortality [22]. It

originates in the lungs' tissues and, if untreated, can metastasize to other organs [23-24]. The majority of lung cancers are carcinomas, with causes ranging from tobacco smoke and air pollution to genetic mutations and single nucleotide polymorphisms (SNPs) [25-26]. Symptoms such as pain, dyspnea, anorexia, fatigue, and cough significantly impact patients' quality of life [27].

Lung cancer remains a global health concern, often detected at advanced stages when the chances of survival are minimal. Approximately 49% to 53% of lung cancer cases are diagnosed at stage 4, where the survival rate is only 6% [29]. Early-stage diagnosis (stage 1) significantly increases the survival rate to 82% [30]. However, early detection remains challenging due to factors like poor image quality, diagnostic complexity, limited diagnostic information, physician fatigue, and inadequate communication. These challenges lead to increased medical costs and deteriorating patient health.

Machine learning offers a promising solution for the early prediction of lung cancer, providing clinicians with a reliable tool for timely diagnosis and intervention. While recent deep learning models have shown commendable results, further improvements are needed to enhance accuracy and robustness. Expanding and refining lung cancer datasets and applying advanced image enhancement techniques are crucial for better diagnostic performance [31-33].

This study focuses on the automatic classification and prediction of lung cancer using CT scans. It aims to distinguish between lung cancer subtypes (adenocarcinoma, large cell carcinoma, squamous cell carcinoma) and healthy individuals. We employ state-of-the-art deep learning models such as ConvNeXt, VGG16, ResNet50, InceptionV3, and EfficientNetB0. Additionally, image enhancement techniques like Histogram Equalization (HE), Contrast Limited Adaptive Histogram Equalization (CLAHE), and noise reduction are applied to improve image quality. Augmentation techniques are also used to enhance dataset robustness and generalization.

By addressing previous limitations, this research aims to develop an accurate and efficient lung cancer prediction model. The proposed approach holds the potential to significantly improve early detection rates, increasing patients' chances of survival and facilitating timely medical intervention.

II. RELATED WORKS

In the last decade, extensive research has focused on using deep learning models to predict lung cancer in its early stages. The abundance of these studies highlights the significance of lung cancer as a research topic. This chapter provides an overview of related works, emphasizing different datasets and methodologies applied by various researchers.

2.1 Related Works with Different Datasets

Ratika et al. [34] evaluated performance scores for daily activities in patients with advanced lung cancer using classification techniques, including Artificial Neural Networks (ANN), Logistic Regression, Naive Bayes, Kernel SVM, KNN, and Random Forest. The results showed that the Random Forest algorithm achieved an accuracy of 88%, while the Artificial Neural Network exhibited the highest prediction accuracy of 89%.

Shaji et al. [35] developed smart computer-aided systems to enhance diagnostic accuracy using machine learning algorithms, including Decision Tree, SVC, Logistic Regression, XGBoost, KNN, Gradient Boosting, and Random Forest. Logistic Regression achieved the highest accuracy of 94%.

Wan [36] implemented visual analysis techniques to explore the distribution and correlation of patient characteristics with lung cancer risk using algorithms like Logistic Regression, KNN, Random Forest, and Decision Tree. Accuracy values ranged from 84% to 90%.

Al-Tawalbeh et al. [37] used machine learning algorithms, including SVM, KNN, Naive Bayes, and Narrow Neural Networks (NNN), to predict lung cancer based on patient symptoms. SVM attained the highest accuracy of 92.6%, while KNN achieved the lowest accuracy at 85.87%.

Zheng et al. [38] proposed a knowledge distillation-based approach, KD_ConvNeXt, combining Swin Transformer and ConvNeXt networks for lung tumor subtype classification. The model achieved a classification accuracy of 85.64% and an F1-score of 0.7717, demonstrating its effectiveness in enhancing accuracy and robustness.

Doppalapudi et al. [39] created multiple survival prediction models using Recurrent Neural Networks (RNN), Convolutional Neural Networks (CNN), and Artificial Neural Networks (ANN). Deep learning models outperformed traditional machine learning models, achieving a classification accuracy of 71.18% and an RMSE of 13.5%.

Chaunzwa et al. [40] applied radiomics techniques using CNNs to predict non-small cell lung cancer (NSCLC) tumor histology from CT data. The best-performing CNN achieved an accuracy of 71% ($p = 0.018$), providing reliable visual explanations for predictions.

Beck et al. [41] applied deep learning algorithms using CNNs for pulmonary nodule detection and classification. Their DeepCUBIT algorithm, which incorporated transfer learning, significantly outperformed a traditional 3D CNN.

Wang et al. [42] introduced a dual-scale categorization (DSC) deep learning method using VGG16 neural networks to evaluate PD-L1 expression. The DSC model achieved an 88% pathologist concordance, surpassing the single-scale method's 83% concordance.

2.2 Related Works with the Same or Similar Datasets

M.G. Lanjewar et al [43], the authors used a deep learning method to classify lung cancer into large cell carcinoma, adenocarcinoma, squamous cell carcinoma, and normal cell using 1000 lung CT scan images from Kaggle. A modified DenseNet201 model with additional layers and feature selection techniques achieved a maximum accuracy of 100% and an average accuracy of 95% using a 5-fold validation technique.

M. Sohaib [44], the authors applied deep learning techniques using VGG16, InceptionV3, and ResNet50 on the Kaggle chest CT scan dataset. The CNN-based model achieved an accuracy of 94.2%, outperforming VGG16 (88.5%), InceptionV3 (91.4%), and ResNet50 (91.4%).

K. Alshamrani et al [45], a collaborative deep learning (CDL) model was proposed to classify cancerous and non-cancerous nodules using ResNet-50 and six feature patches. Trained on 1000 lung CT scan images from Kaggle, the CDL model demonstrated a high accuracy of 93.24%.

M. R. Ankoliya et al [46], the authors focused on classifying lung cancer cells into adenocarcinoma, large cell carcinoma, squamous cell carcinoma, or normal cells using NFNet and EfficientNetB4. The NFNet model achieved a classification accuracy of 96%, while EfficientNetB4 achieved 94%.

H. F. Kareem [47], a computer system using image processing and computer vision methods was proposed to classify lung cancer into normal, benign, or malignant categories. The model, trained on 1100 lung CT scan images from two Iraqi hospitals and the IQ-OTH/NCCD Kaggle dataset, achieved a classification accuracy of 89.8% using an SVM classifier.

A. Campanella [48], a computer-aided system using AlexNet CNN architecture was introduced for lung cancer detection. Using over 1100 lung CT scan images from the IQ-OTH/NCCD Kaggle dataset, the model achieved a high accuracy of 93.5%.

III. METHODOLOGY

3.1 Proposed System

This chapter presents the study's workflow, illustrated in Figure 1, which begins with data loading and concludes with the development and training of predictive models for lung cancer diagnosis. It covers the data loading process, the application of image enhancement techniques, and the data preprocessing steps. Furthermore, the construction of predictive models designed for lung cancer diagnosis is described in detail (refer to Figure 2).

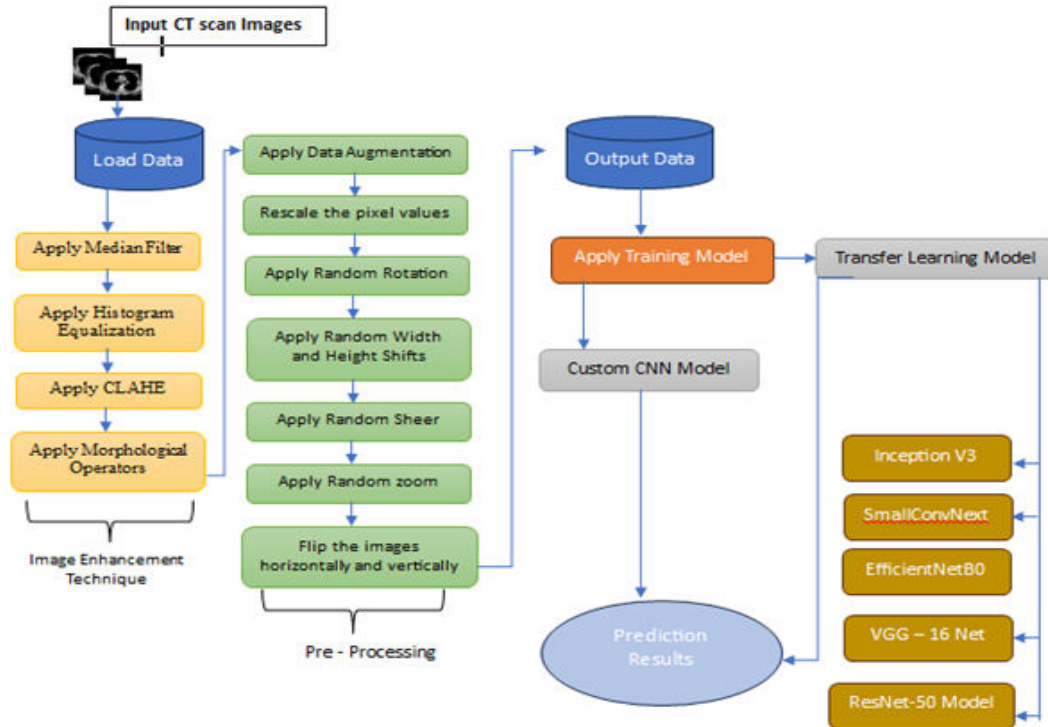


Fig. 1. Study Flow chart.

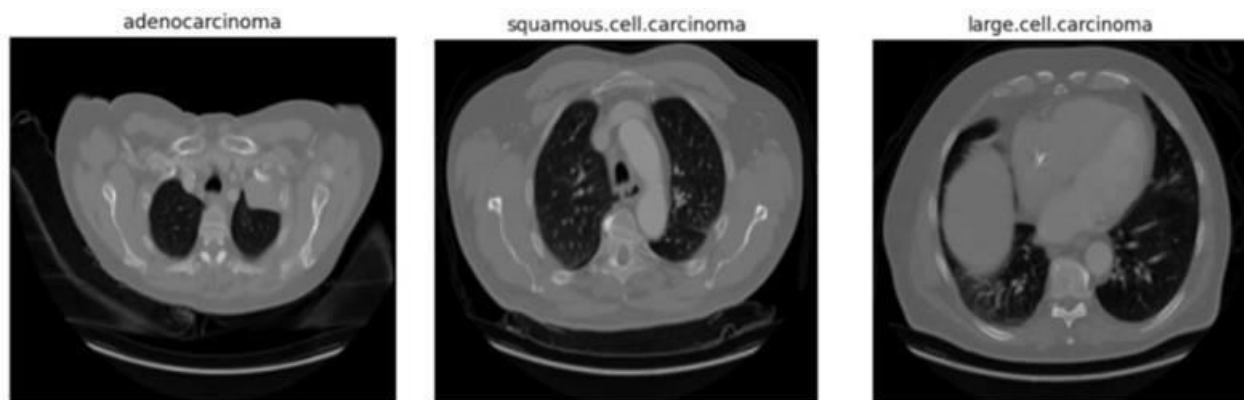


Fig. 2. CT scan images for lung cancer patients with it types taken from the Dataset .

3.2 Data loading

The dataset used in this study is sourced from Kaggle, a widely recognized platform offering a variety of datasets for data science applications. Specifically, it comprises the "Chest CT-Scan Images Dataset," curated by researcher Mohammad Hany to support medical imaging analysis, with a focus on lung diseases. The dataset contains 1,000 CT scan images in .png and .jpg formats, representing different types of lung cancer. It is organized into three subsets: training, testing, and validation. The images are categorized into four classes: Adenocarcinoma, Large Cell Carcinomas, Squamous Cell Carcinomas, and Normal Cells. Additionally, the dataset provides visual examples of various lung cancers alongside comparisons with non-lung cancer images.

3.3. Image enhancement techniques

CT images often experience degradation due to factors such as noise, low contrast, and blurring, which can diminish their clarity and hinder accurate representation. These challenges are commonly associated with low radiation doses and inadequate enhancement algorithms. To enhance CT image quality, various techniques can be applied to reduce noise, improve contrast, and optimize overall clarity. Achieving optimal results requires careful selection and adjustment of these techniques, considering the specific characteristics of the images and the desired level of enhancement. Effective medical image enhancement methods, including histogram equalization (HE) and contrast-limited adaptive histogram equalization (CLAHE), play a crucial role in improving image visibility and providing detailed information, thereby assisting physicians in making accurate diagnoses (refer to Figure 3).

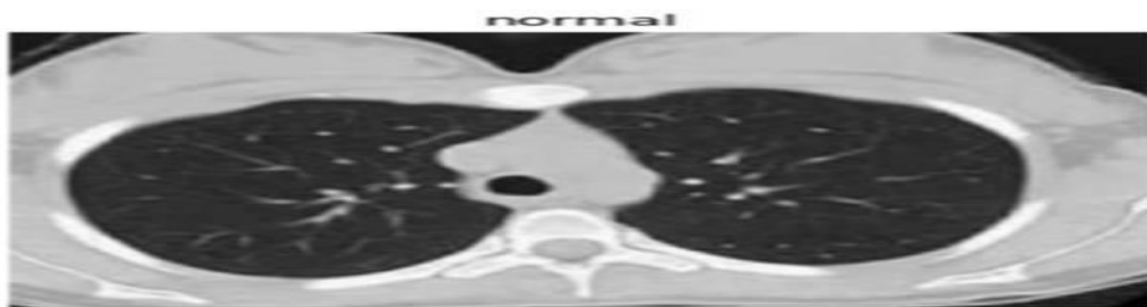


Fig. 3. CT scan image for non-lung cancer patient taken from the Dataset .

3.3.1 Median Filter (MF): The median filter is a noise reduction technique that replaces anomalous pixel values with the median value of the surrounding pixels, effectively eliminating salt-and-pepper and Gaussian noise. It serves as a useful preprocessing step for CT scan images, reducing noise and enhancing image quality to facilitate further analysis. By applying the median filter, the clarity and visibility of critical features are improved. Figure 4 presents a comparison of a sample CT scan image from the dataset before and after the application of the median filter technique.

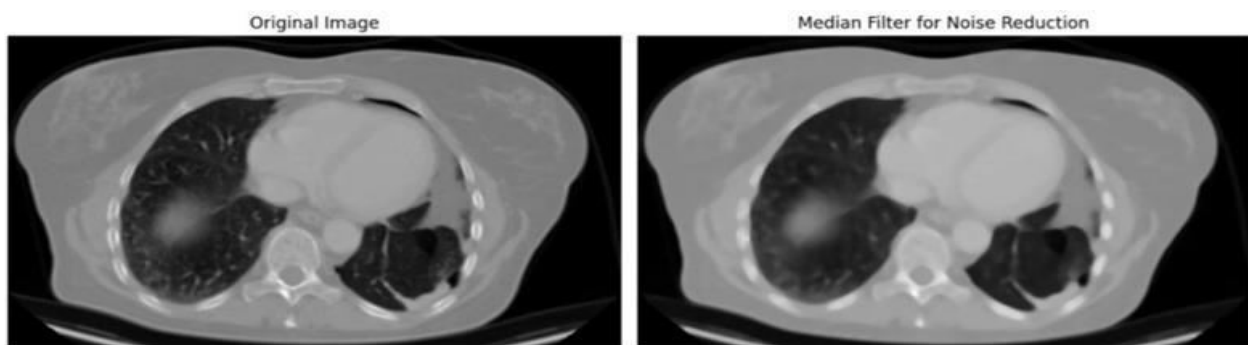


Fig. 4. CT scan image before and after applying the MF technique .

3.3.2. Histogram Equalization (HE): Histogram Equalization (HE) is a contrast enhancement technique that improves the visibility of structures and details within an image by redistributing pixel values to expand the dynamic range of the histogram. It is particularly effective for enhancing low-contrast images like CT scans. When applied following noise reduction, HE can substantially improve the overall image appearance, making it more suitable for analysis. Figure 5 illustrates a CT scan image from the dataset before and after the application of the Histogram Equalization technique.

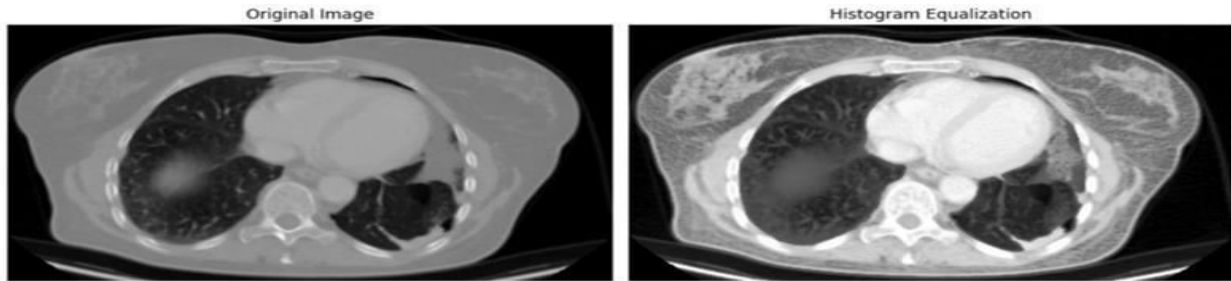


Fig. 5. CT scan image before and after applying the HE technique .

3.3.3. Contrast Limited Adaptive Histogram Equalization (CLAHE): Contrast Limited Adaptive Histogram Equalization (CLAHE) is an advanced contrast enhancement technique that improves image details by dividing the image into small regions, known as tiles. It is often applied after Histogram Equalization to further enhance specific areas of an image. The CLAHE process involves five steps: histogram adjustment, application of a mapping function, and bilinear interpolation to smooth transitions and eliminate block artifacts. Typically, the image is divided into 64 blocks, each measuring 8x8 pixels, to ensure localized contrast enhancement. Additionally, CLAHE prevents noise amplification by limiting contrast in homogeneous regions. Figure 6 presents a CT scan image from the dataset before and after applying the CLAHE technique.

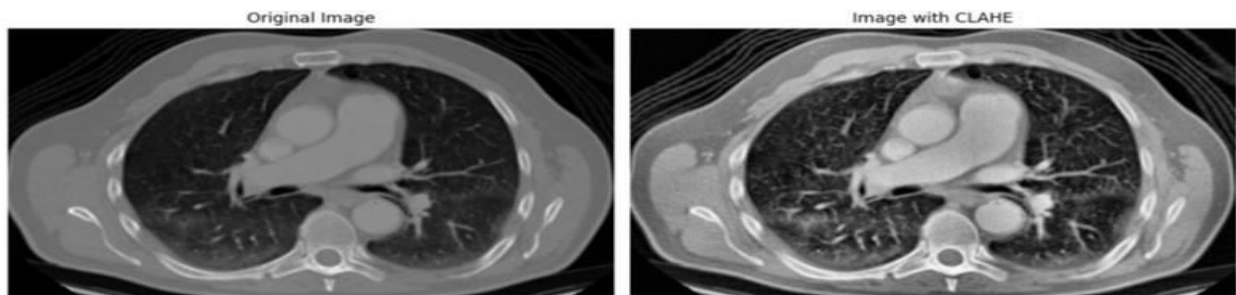


Fig. 6. CT scan image before and after applying the CLAHE technique .

3.3.4. Morphological Operators (MO): Morphological operations are effective techniques for further enhancing image details and contrast, particularly after applying CLAHE. Dilation enhances the visibility of features by expanding object boundaries and filling in small gaps, while Erosion removes minor objects and noise, leaving only significant features. By combining these operations, edge detection is refined, contributing to improved image clarity. Morphological operations are widely used in medical imaging to sharpen images, often employing gradient-based operators alongside morphological filters to detect and enhance edges. Figure 7 showcases a CT scan image from the dataset before and after the application of Dilation and Erosion techniques.



Fig. 7. CT scan image before and after applying the Dilation and Erosion techniques .

3.4 Data pre-processing:

3.4.1 Data augmentation: Data augmentation is employed to enhance the volume and diversity of training data for lung cancer detection using CT scan images. This technique helps fine-tune model parameters, bridge the gap between training and validation sets, and reduce validation errors, particularly when dealing with small datasets and variations in image acquisition. In this study, several augmentation strategies are applied:

- **Resizing:** CT scan images are adjusted to a fixed size of 224x224 pixels to improve computational efficiency and ensure uniformity.
- **Shear Range:** A 20% shear transformation is applied to enhance the model's robustness in detecting lesions at different angles.
- **Horizontal Flip:** Images are flipped horizontally, enabling the model to recognize lesions from various orientations.
- **Vertical Flip:** Images are flipped vertically to further improve the model's ability to identify lung lesions.
- **Rescale:** Pixel values are normalized to a range of 0 to 1, aiding the model in learning robust features and reducing the risk of overfitting.

3.5 Models building

This section describes the development of predictive models for lung cancer diagnosis using the provided dataset. An Enhanced Convolutional Neural Network (CNN) was designed and implemented, along with the utilization of several pre-trained models, including ConvNeXtSmall, VGG16, ResNet50, InceptionV3, and EfficientNetB0. To ensure balanced representation, the dataset consisting of 1,000 CT scans was randomly shuffled and divided into training, testing, and validation sets of varying sizes. The distribution of these subsets is illustrated in Fig. 8.

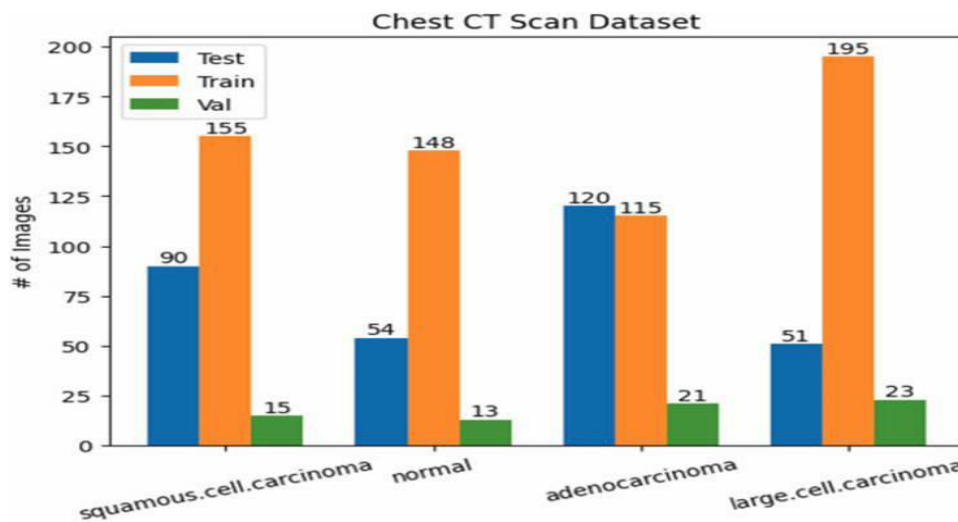


Fig. 8. Training, testing, and validating data distribution for each type .

3.5.1. Enhanced CNN model architecture: Convolutional Neural Networks (CNNs) are a specialized type of neural network particularly well-suited for image classification tasks and visual imagery analysis. They have proven highly effective in various applications, including object recognition, image classification, and medical image analysis, making them ideal for identifying lung cancer in CT scan images.

This study introduces a customized multi-class lung abnormality classifier using a tailored CNN architecture consisting of eight layers:

1. **Layer 1:** A convolutional layer with **64 filters (3x3)** and **ReLU activation** to extract features from input images of shape **(224, 224, 3)**. It is followed by a **max-pooling layer (2x2)** to reduce spatial dimensions.

2. **Layer 2:** Another convolutional layer with **32 filters (3x3)** and **ReLU activation**, followed by a **max-pooling layer (2x2)** for further dimensionality reduction.
3. **Layer 3:** A third convolutional layer with **32 filters (3x3)** and **ReLU activation**, followed by a **dropout layer (rate = 0.4)** to prevent overfitting.
4. **Layer 4:** An additional **dropout layer** to further mitigate overfitting.
5. **Layer 5:** The output from the previous convolutional layers is flattened into a **1D array** to prepare it for the dense layers.
6. **Layer 6:** A **dense layer with 256 neurons** and **ReLU activation** extracts complex features. A **dropout layer (rate = 0.4)** follows to reduce overfitting.
7. **Layer 7:** A second **dense layer with 128 neurons** and **ReLU activation** for further feature extraction.
8. **Layer 8:** The final **dense layer** comprises **4 neurons** with a **SoftMax activation function**, producing a probability distribution across the four output classes (Adenocarcinoma, Large Cell Carcinomas, Squamous Cell Carcinomas, and Normal Cells).

The detailed architecture of the proposed CNN model is visually represented in **Figure 9**.

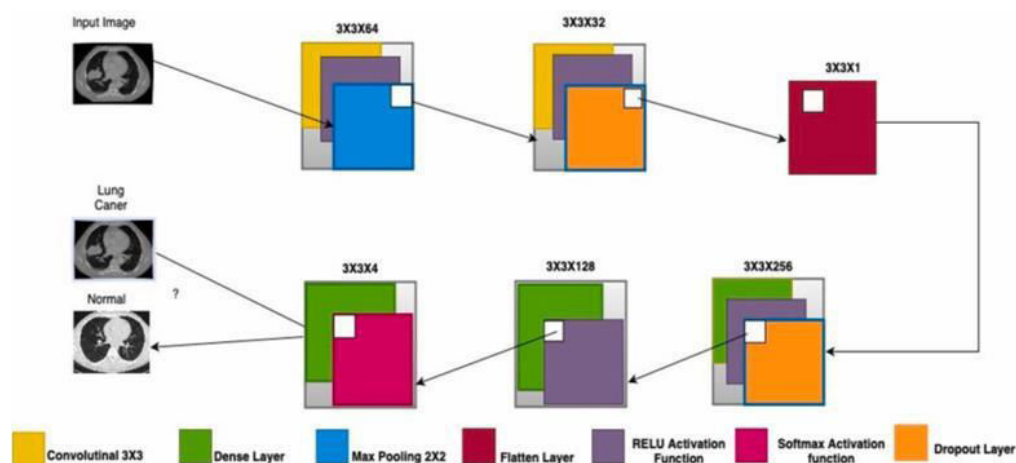


Fig. 9. Enhanced CNN model architecture of lung cancer prediction.

3.5.2. ConvNeXtSmall model architecture: Facebook AI Research (FAIR) introduced **ConvNeXt** in 2022 as a next-generation convolutional neural network (CNN) architecture. It has gained significant popularity in recent years, particularly for computer vision tasks like object detection and image classification.

ConvNeXtSmall is a pre-trained variant of the ConvNeXt architecture designed for efficient performance. It consists of **50 layers** and incorporates advanced techniques such as **depth-wise separable convolutions** and **channel shuffle** to optimize feature extraction. Additionally, the model employs **pooling layers** to reduce spatial dimensions and uses **two fully connected (FC) layers** for classification, producing output values between **0 and 4** to indicate the presence and type of lung cancer.

In this study, **ConvNeXtSmall** was used as the base model and further enhanced by adding:

- **Dropout layers** to reduce overfitting.
- **Batch normalization layers** for faster training and better generalization.
- **Dense layers with ReLU activation** for additional feature extraction and classification.

The model was compiled using the **Adam optimizer** and the **categorical cross-entropy loss function**, and it was trained for **150 epochs**. The detailed architecture of the improved ConvNeXtSmall model is illustrated in **Figure 10**.

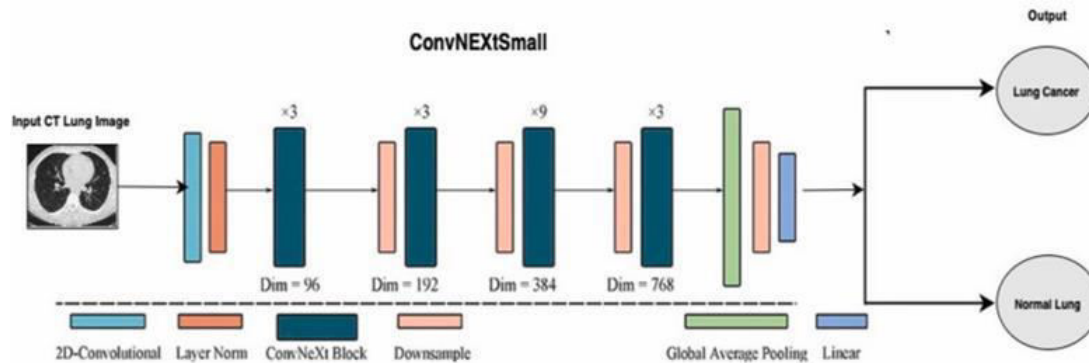


Fig. 10. ConvNeXtSmall model architecture of lung cancer prediction .

3.5.3. ResNet50 model architecture: In 2015, Microsoft Research introduced the **Residual Neural Network (ResNet)** architecture to address the issue of vanishing gradients in deep neural networks. **ResNet50** is a specific version of this architecture, consisting of **50 layers** and incorporating **residual connections** that enable the efficient training of deeper networks by facilitating gradient flow.

In this study, **ResNet50** was employed as a **pre-trained model** for lung cancer prediction due to its robust feature extraction capabilities. The model comprises:

- **Fifty convolutional layers** for extracting features.
- **One pooling layer** for reducing spatial dimensions and computational complexity.
- **Two fully connected (FC) layers** for classification.

The pooling layer not only reduces the number of parameters but also prevents overfitting, while the convolutional layers capture meaningful features from the input images. The FC layers classify the images based on the extracted features.

During the initial training phase, **70%** of the lung scans were used for training, and the remaining **30%** were used for evaluation. The model was compiled using the **binary cross-entropy loss function** and optimized using the **Adam optimizer**. It was trained for **150 epochs**.

For classification, the model applies filters to the input images, and the **SoftMax layer** produces output values between **0 and 1**, representing the likelihood of lung cancer presence. The architecture and working of the ResNet50 model in this study are illustrated in **Figure 11**.

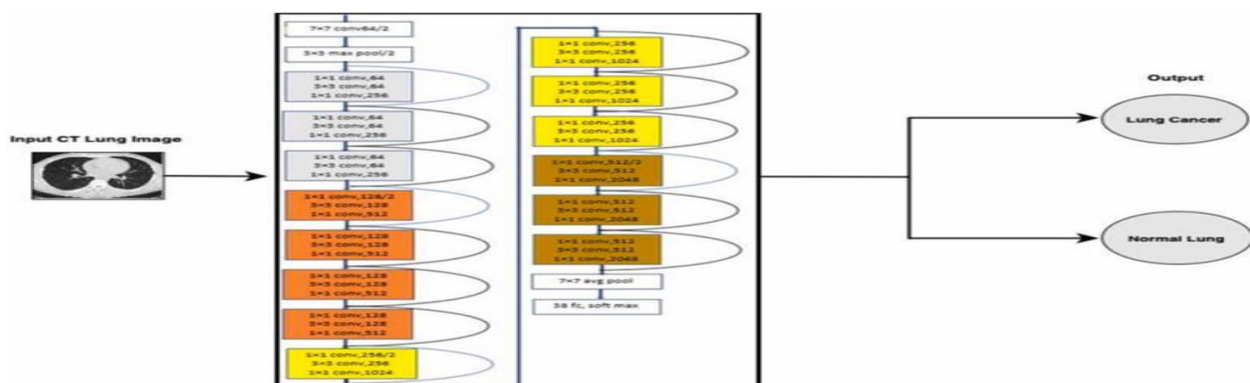


Fig. 11. ResNet50 model architecture of Lung cancer prediction .

3.5.4. VGG16 model architecture: The VGG16 model, consisting of **16 trainable weight layers** (13 convolutional layers and 3 fully connected layers), is well-regarded for its simplicity and effectiveness. It uses **3x3 convolutional filters** with a **stride of 1** and **padding of 1** to extract fine details from input images.

VGG16 is particularly effective in image recognition tasks and is widely applied in medical imaging, including **CT scans** and **chest X-rays**. Its deep convolutional network design allows it to identify intricate patterns indicative of lung cancer, such as nodules or tumors.

In this study, VGG16 was utilized as a **pre-trained model** for lung cancer prediction. The initial layers were **frozen** to retain the pre-learned low-level features, while the prediction layers were fine-tuned for classification. The model's architecture consists of:

- **Five convolutional blocks** with convolutional and pooling layers.
- **Fully connected dense layers** with ReLU activation.
- **Dropout layers** to reduce overfitting.
- A **SoftMax layer** to predict the cancer class probabilities.

The dataset was divided into **70% for training** and **30% for validation**, using the **Adam optimizer** and **categorical cross-entropy loss function**. To mitigate overfitting, **early stopping** with a patience of **20 epochs** was applied. The model's performance was assessed using metrics such as **accuracy, precision, recall, and loss**. The architecture of VGG16 used in this study is illustrated in **Figure 12**.

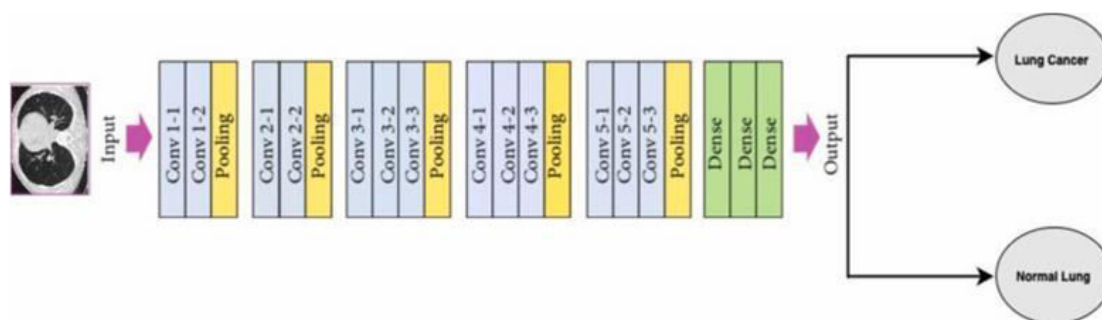


Fig. 12. VGG16 model architecture of Lung Cancer prediction .

3.5.5. EfficientNetB0 model architecture: EfficientNet has established itself as a top-performing convolutional neural network (CNN) architecture, delivering high accuracy with significantly lower computational demands and fewer parameters compared to other state-of-the-art models. Its unique scaling method uniformly balances network depth, width, and resolution, making it especially suitable for environments with limited computing resources, such as embedded systems or mobile devices.

In this study, **EfficientNetB0** was chosen as a **pre-trained base model** for lung cancer classification due to its excellent accuracy and computational efficiency in image-based tasks. To enhance its robustness and address overfitting, the following modifications were applied:

- **GlobalAveragePooling2D Layer:** Reduces the spatial dimensions and extracts global features.
- **Dropout Layer:** Prevents overfitting by randomly dropping nodes during training.

The model was trained using **70% of the lung CT-scan image dataset** and evaluated on the remaining **30%**. The **Adam optimizer** and **categorical cross-entropy loss function** were applied. EfficientNetB0 is designed for **224x224x3** input images, employing multiple convolutional layers with a **3x3 receptive field** for effective feature extraction. The model was trained for **100 epochs**.

The detailed architecture of the **EfficientNetB0** model used in this study is illustrated in **Figure 13**.

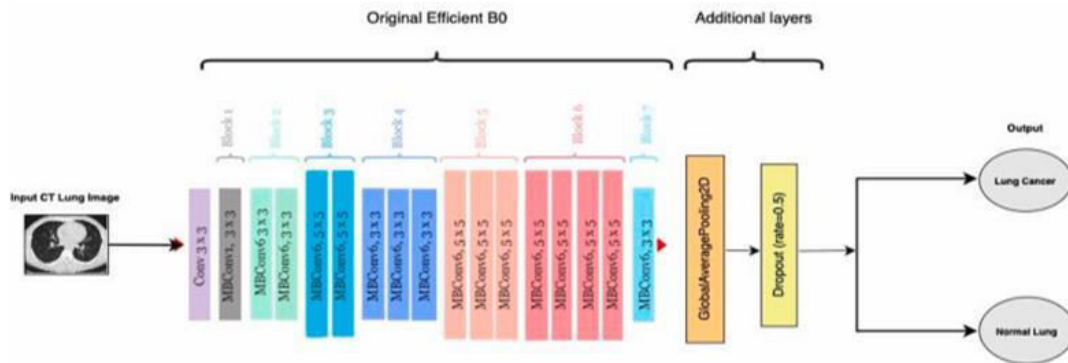


Fig. 13. EfficientNetB0 Modified model architecture of Lung Cancer prediction [70].

3.5.6. InceptionV3 model architecture: InceptionV3 has proven to be an invaluable resource in **computer vision applications** like object detection, recognition, segmentation, and image captioning. Its robust feature extraction capabilities make it particularly effective for interpreting **medical images**, including CT scans for lung cancer diagnosis.

In this study, **InceptionV3** was applied as a **pre-trained framework** for lung cancer prediction. To leverage its prior knowledge, the initial layers were **frozen**, focusing the training process on the prediction layers. The architecture consists of **92 layers**, comprising convolutional, pooling, and concatenation operations. The final layer uses a **SoftMax activation function** to generate a **probability score** for classification, determining whether a lung is cancerous or normal.

The model was trained using **70% of the dataset** and evaluated on the remaining **30%**. Training utilized the **Adam optimizer** and **categorical cross-entropy loss function** over **150 epochs**. **Early stopping** was applied to prevent overfitting, terminating training if the validation loss remained unchanged for **20 consecutive epochs**. The successful classification performance of the **InceptionV3** model in identifying lung cancer from CT scan images is visually represented in **Figure 14**.

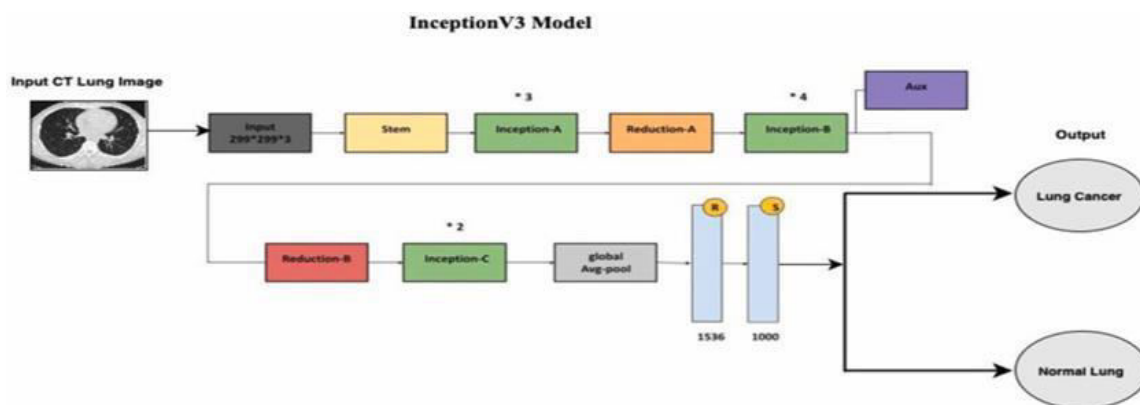


Fig. 14. InceptionV3 model architecture of Lung Cancer prediction .

IV. EXPERIMENTS AND RESULTS

To achieve the study's objectives, two experiments were conducted to detect lung cancer using chest CT scan images. The first experiment involved developing an Enhanced Convolutional Neural Network (CNN) from scratch, focusing on effective feature extraction and classification. The second experiment utilized five state-of-the-art pre-trained models — ConvNeXtSmall, VGG16, ResNet50, InceptionV3, and EfficientNetB0 — which were fine-tuned for the

specific dataset using transfer learning techniques. These models were enhanced with additional layers to improve classification accuracy. Model performance was evaluated using a dedicated testing dataset to ensure reliability and robustness. The experiments were implemented in Python, known for its simplicity and versatility in machine learning applications, using libraries like TensorFlow and Keras. The computations were carried out on the Kaggle platform, which offers extensive computational resources and access to diverse datasets, facilitating efficient model training and evaluation.

4.1. Experiment dataset

This study utilized a dataset comprising four distinct classes of lung cancer: adenocarcinoma (338 images), large cell carcinoma (187 images), squamous cell carcinoma (260 images), and normal (215 images). To facilitate effective model training and evaluation, the dataset was divided into three subsets: 70% for training, 20% for testing, and 10% for validation, as outlined in Table 1. This systematic distribution ensured that the models could effectively learn meaningful features from the training data while maintaining a reliable evaluation process. Figure 15 showcases representative features from the training dataset, capturing the diversity of lung cancer manifestations, whereas the Figure 16 illustrates samples from the testing dataset, highlighting the variability in image characteristics used for model assessment.

Table 1. The Percentages and Number of images in the training, testing, and validating dataset.

Dataset	Number of Images	Splitting percentage
Training set	613	70 %
Testing set	315	20 %
Validating set	72	10 %

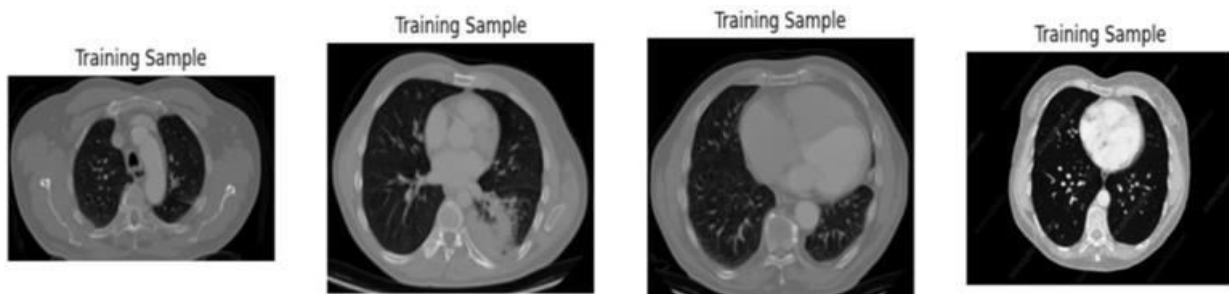


Fig. 15. Sample of CT scan images from the training dataset.

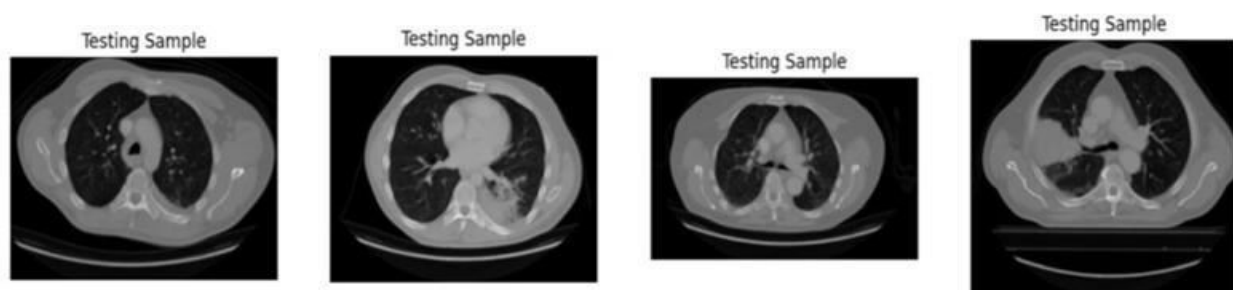


Fig. 16. Sample of CT scan images from the testing dataset

4.2. Hyperparameters

To optimize model performance, a specific set of hyperparameters was carefully chosen. The training process involved running for 150 epochs, incorporating early stopping to mitigate overfitting by monitoring validation loss. Training was

halted if no improvement was observed after 20 epochs. While most models used a default input size of 224x224, the ConvNeXt model employed an increased size of 256x256 to explore potential performance enhancements. The Adam optimizer, with a standard learning rate, ensured stable and efficient training. Evaluation metrics included categorical cross-entropy loss, accuracy, precision, and recall, providing comprehensive insights into model effectiveness. These hyperparameters were instrumental in achieving high-quality classification results. The detailed training hyperparameters and loss functions are summarized in Table 2.

Table 2. Training hyperparameters and loss function for training.

Hyperparameter	Value
Optimizer	Adam
Loss function	categorical_crossentropy
Metrics	accuracy, precision, recall
Early Stopping	True
Patience	20
Number of epochs	50
Batch size	(default: 32)

4.3. Performance evaluation metrics

The models' performance was assessed using a confusion matrix, a reliable tool for evaluating classification accuracy. In this study, four classes were considered: adenocarcinoma, large-cell carcinoma, squamous cell carcinoma, and normal lung tissue. The confusion matrix provides a clear summary of the model's predictions, displaying the number of True Positives (TP), True Negatives (TN), False Positives (FP), and False Negatives (FN) for each class. True Positives indicate correct predictions for specific cancer types or normal tissue, while True Negatives represent accurate non-cancer predictions. False Positives and False Negatives correspond to incorrect predictions, reflecting areas where the model may require further refinement. Table 3 presents the detailed confusion matrix used to evaluate the models' classification performance.

Table 3. Confusion Matrix

Empty Cell	Predictive Class Positives	Predictive Class Negative
Actual Class Positives	True Positive (TP)	False Negative (FN)
Actual Class Negative	False Positive (FP)	True Negative (TN)

We used four key metrics—accuracy, precision, recall, and F1-score—to evaluate the performance of our classification model for predicting four classes: adenocarcinoma, large cell carcinoma, squamous cell carcinoma, and normal tissue. These metrics are defined as follows:

- Accuracy: measures the proportion of correctly classified instances (Equation (1)).
- Recall: indicates the proportion of true positive predictions among actual positive cases (Equation (2)).
- Precision: represents the proportion of true positive predictions among all positive predictions (Equation (3)).
- F1-Score: is the harmonic mean of precision and recall, providing a balanced assessment (Equation (4)).

$$\text{Accuracy} = \frac{TP}{(TP + FP)} \text{ --- (1)}$$

$$\text{Recall} = \frac{TP}{(TP + FN)} \text{ --- (2)}$$

$$\text{Precision} = \frac{TP}{(TP + FP)} \text{ --- (3)}$$

$$\text{F1 - Score} = \left(\frac{2 * \text{Precision} * \text{Recall}}{\text{Precision} + \text{Recall}} \right) \text{ --- (4)}$$

These metrics offer a comprehensive evaluation of the model's predictive capabilities. Collectively, they evaluate the model's reliability and effectiveness in clinical applications where accurate diagnosis is essential.

4.4. Models results:

After training the models using the training dataset, their performance was evaluated on the testing and validation datasets, which comprised 30% of the images. The assessment was conducted using key metrics: accuracy, recall, precision, and F1-score. These metrics were calculated to assess the effectiveness of the models in classifying lung cancer cases accurately.

Table 4 compares the performance of various models for lung cancer diagnosis. The Enhanced CNN model stands out with exceptional results, achieving 100% accuracy, 99.2% precision, 98.0% recall, and an F1-score of 98.4%, demonstrating its superior ability to detect cases while minimizing false predictions. VGG16 followed with a strong performance, attaining 99% accuracy and consistently high scores across precision and F1-score. EfficientNetB0 also delivered reliable results, achieving the highest precision at 99.5% and maintaining a solid recall score.

On the other hand, ResNet50 presented moderate outcomes, with comparatively lower recall. ConvNeXt showed a balanced performance, though its overall scores were lower than the leading models. InceptionV3 ranked the lowest, exhibiting significantly reduced precision and accuracy, highlighting its limitations in this study's classification task.

Figure 17 visually compares the accuracy of the different models. The results underscore the Enhanced CNN model's effectiveness, surpassing traditional deep learning models with its perfect accuracy. In comparison, VGG16 and EfficientNetB0 demonstrated robust performance with accuracies of 99% and 97.9%, respectively, emerging as the top-performing pre-trained models. These findings suggest that the proposed Enhanced CNN model is particularly reliable for lung cancer diagnosis, while the other pre-trained models still offer valuable accuracy for practical applications.

Table 4: Comparison of the performance of various models for lung cancer diagnosis.

Models	Precision (%)	Recall (%)	F1-Score (%)	Accuracy (%)
Enhanced CNN	99.2 %	98.0 %	98.4 %	99.09 %
ConvNeXt	86.7 %	89.5 %	88.0 %	87 %
VGG16	99.1 %	98.4 %	99.6 %	99 %
ResNet50	93.1 %	76.4 %	85.2 %	94.5 %
InceptionV3	48.5 %	93.2 %	77.1 %	76.9 %
EfficientNetB0	99.5 %	99.2 %	99.6 %	97.9 %

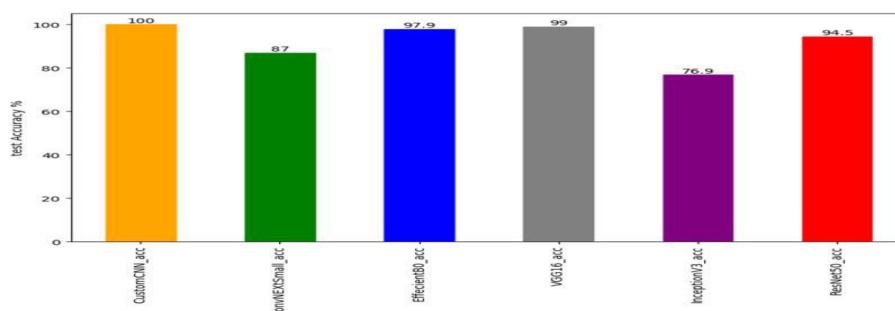


Fig. 17. Comparison of Performance Accuracy for all models.

Figure 18 presents the accuracy and loss curves for the proposed Enhanced CNN model during testing and validation. The model achieved an exceptional accuracy of 99.09%, with a continuous decline in loss, reflecting its robust performance. The gradual reduction in the loss metric, which measures the disparity between predicted and actual values, indicates the model's strong learning capability and effective generalization.

Figure 19 displays the accuracy and loss curves for the ConvNeXtSmall model during training and validation. The model attained a final accuracy of 86%, with a consistent reduction in loss over the training and testing phases. This stable convergence suggests the model's reliability and good generalization capabilities.

Figure 20 showcases the accuracy and loss curves for the VGG16 model. Achieving a remarkable accuracy of 99%, the model demonstrated strong performance with a steady decrease in loss, confirming its ability to accurately classify lung cancer cases.

Figure 21 illustrates the accuracy and loss curves for the ResNet50 model. The model reached a high accuracy of 94.5%, with a visible decline in loss, indicating effective learning. While its accuracy was slightly lower than that of VGG16 and Enhanced CNN, ResNet50's performance remains commendable.

Figure 22 presents the accuracy and loss curves for the InceptionV3 model. The model achieved an accuracy of 76.9%, with a gradual reduction in loss. Although its accuracy was comparatively lower, the consistent decrease in loss indicates a reasonable learning process and potential for improvement.

Figure 23 displays the accuracy and loss curves for the EfficientNetB0 model, which also achieved an accuracy of 76.9%. The model exhibited a stable decrease in loss during training and validation, demonstrating satisfactory learning performance. While its accuracy was lower than other models, it still performed reasonably well given its computational efficiency.

These visual representations provide a comprehensive understanding of how each model learned and performed, with the Enhanced CNN and VGG16 models standing out as the most effective in accurately predicting lung cancer.

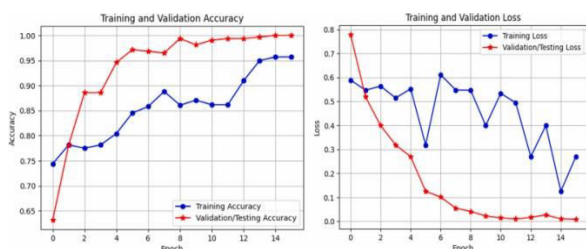


Fig. 18. The Enhanced CNN model Accuracy and Loss during training and testing.

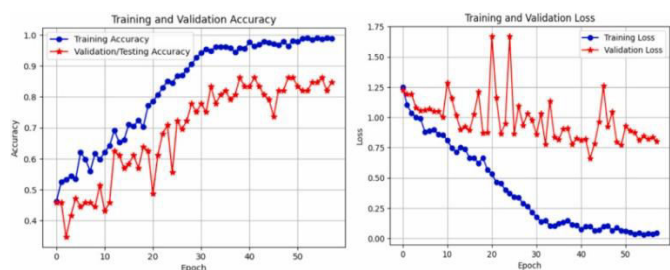


Fig. 19. The ConvNeXtSmall model Accuracy and Loss during training and testing.

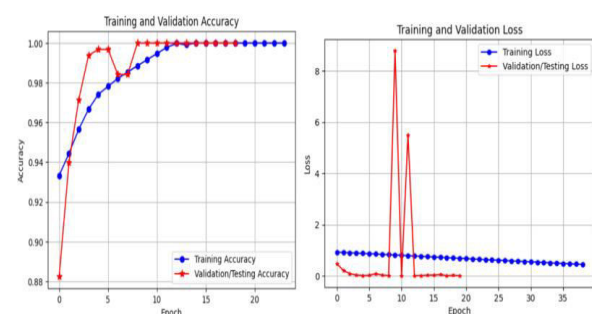


Fig. 20. The VGG16 model Accuracy and Loss during training and testing.

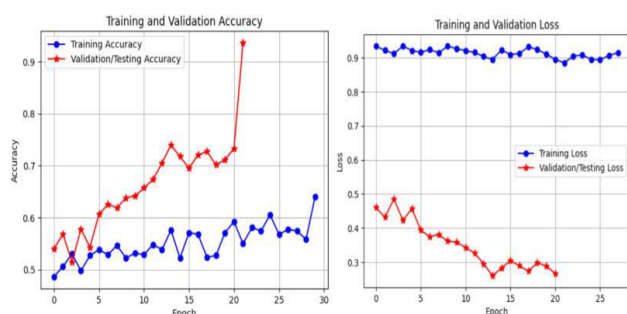


Fig. 21. The ResNet50 model Accuracy and Loss during training and testing.

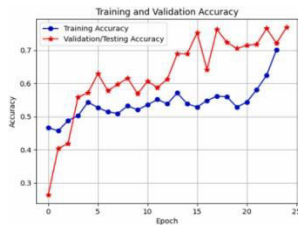


Fig. 22. The InceptionV3 model Accuracy and Loss during training and testing.

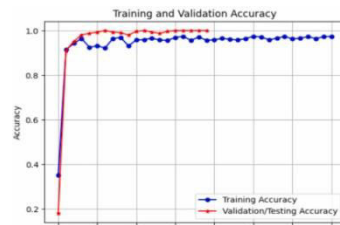
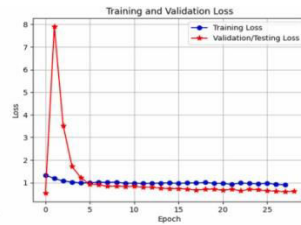
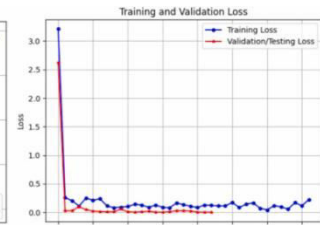


Fig. 23. The EfficientNetB0 model Accuracy and Loss during training and testing.



V. CONCLUSION

Lung cancer continues to pose a substantial global health challenge, accounting for approximately 13-14% of all cancer diagnoses and exhibiting particularly high mortality rates in its later stages. Early detection remains crucial for improving survival outcomes, yet traditional diagnostic methods are often limited by factors such as inadequate image quality, physician fatigue, and low diagnostic accuracy. These limitations highlight the urgent need for advanced, automated solutions to enhance early diagnosis and support more effective treatment planning. In this study, we present a novel approach for the automated classification and prediction of lung cancer using chest CT scan images. A dataset comprising 1,000 CT scans was obtained from Kaggle, representing four distinct categories: Adenocarcinoma, Large Cell Carcinoma, Squamous Cell Carcinoma, and Normal. To address the complexities of lung cancer classification, we developed a customized Convolutional Neural Network (CNN) model that demonstrated exceptional performance, achieving a testing accuracy of 99.09%. Furthermore, we incorporated enhancement techniques and leveraged the ConvNeXt model to further refine performance, resulting in significant improvements over existing models in lung cancer detection. This innovative approach underscores the potential of deep learning in revolutionizing early cancer diagnosis, offering a reliable and efficient tool for medical professionals in their diagnostic decision-making processes.

REFERENCES

- [1] M. F. A. Zaharuddin, D. Kim, and S. Rhee, "An ANFIS based approach for predicting the weld strength of resistance spot welding in artificial intelligence development," *Journal of Mechanical Science and Technology*, vol. 31, no. 11, pp. 5467–5476, Nov. 2017, doi: 10.1007/S12206-017-1041-0.
- [2] Z. Xin, Z. Yansong, and C. Guanlong, "Model optimization of artificial neural networks for performance predicting in spot welding of the body galvanized DP steel sheets," in *Lecture Notes in Computer Science*, vol. 4221, pp. 602–605, 2006, doi: 10.1007/11881070_82.
- [3] H. W. Loh, C. P. Ooi, S. Seoni, P. D. Barua, F. Molinari, and U. R. Acharya, "Application of explainable artificial intelligence for healthcare: a systematic review of the last decade (2011–2022)," *Computer Methods and Programs in Biomedicine*, vol. 226, Article 107161, Nov. 2022, doi: 10.1016/J.CMPB.2022.107161.
- [4] K. H. Yu, A. L. Beam, and I. S. Kohane, "Artificial intelligence in healthcare," *Nature Biomedical Engineering*, vol. 2, no. 10, pp. 719–731, Oct. 2018, doi: 10.1038/s41551-018-0305-z.
- [5] "REVIEW: Evaluation of artificial intelligence tools for diagnostic or predictive analysis," Park and Han, doi: 10.1148/radiol.2017171920.
- [6] M. L. Giger, "Machine learning in medical imaging," *Journal of the American College of Radiology*, vol. 15, no. 3, pp. 512–520, Mar. 2018, doi: 10.1016/J.JACR.2017.12.028.
- [7] A. Elaraby, "Quantum medical images processing foundations and applications," *IET Quantum Communication*, 2022, doi: 10.1049/QTC2.12049.
- [8] S. K. Baduge et al., "Artificial intelligence and smart vision for building and construction 4.0: Machine and deep learning methods and applications," *Automation in Construction*, vol. 141, Article 104440, Sep. 2022, doi: 10.1016/J.AUTCON.2022.104440.
- [9] Z. Y. G. Ko, Y. Li, J. Liu, H. Ji, A. Qiu, and N. Chen, "DOTnet 2.0: Deep learning network for diffuse optical tomography image reconstruction," *Intelligent Based Medicine*, vol. 9, Article 100133, Jan. 2024, doi: 10.1016/J.IBMED.2023.100133.
- [10] C. Janiesch, P. Zschech, and K. Heinrich, "Machine learning and deep learning," *Electronic Markets*, vol. 31, no. 3, pp. 685–695, Sep. 2021, doi: 10.1007/S12525-021-00475-2.

- [11] D. D. Martinelli, "Machine learning for metabolomics research in drug discovery," *Intelligent Based Medicine*, vol. 8, Article 100101, Jan. 2023, doi: 10.1016/J.IBMED.2023.100101.
- [12] I. Pacal, D. Karaboga, A. Basturk, B. Akay, and U. Nalbantoglu, "A comprehensive review of deep learning in colon cancer," *Computers in Biology and Medicine*, vol. 126, Article 104003, Nov. 2020, doi: 10.1016/J.COMPBIOMED.2020.104003.
- [13] B. Sahiner et al., "Deep learning in medical imaging and radiation therapy," *Med. Phys.*, vol. 46, no. 1, pp. e1-e36, Jan. 2019, doi: 10.1002/MP.13264.
- [14] T. A. Retson and M. Eghtedari, "Computer-aided detection/diagnosis in breast imaging: a focus on the evolving FDA regulations for using software as a medical device," *Curr. Radiol. Rep.*, vol. 8, no. 6, pp. 1-7, Jun. 2020, doi: 10.1007/S40134-020-00350-6.
- [15] R. A. Alharbi, "Impact of different types of cancer on health-related quality of life," *Pak. J. Med. Health Sci.*, vol. 16, no. 4, p. 762, May 2022, doi: 10.53350/PJMHS22164762.
- [16] H. K. Kim, T. W. Ha, and M. R. Lee, "Single-cell transcriptome analysis as a promising tool to study pluripotent stem cell reprogramming," *Int. J. Mol. Sci.*, vol. 22, no. 11, p. 5988, Jun. 2021, doi: 10.3390/IJMS22115988.
- [17] A. Fadaka, B. Ajiboye, O. Ojo, O. Adewale, I. Olayide, and R. Emuowhochere, "Biology of glucose metabolism in cancer cells," *J. Oncol. Sci.*, vol. 3, no. 2, pp. 45-51, Jul. 2017, doi: 10.1016/J.JONS.2017.06.002.
- [18] Y. He et al., "Targeting PI3K/Akt signal transduction for cancer therapy," *Signal Transduct. Targeted Ther.*, vol. 6, no. 1, pp. 1-17, Dec. 2021, doi: 10.1038/s41392-021-00828-5.
- [19] U. Biswas and J. K. Rakshit, "Photonic crystal race track ring resonator design for the detection of cancer cells," *J. Phys. Conf. Ser.*, vol. 2335, no. 1, Article 012004, Sep. 2022, doi: 10.1088/1742-6596/2335/1/012004.
- [20] M. R. Abbasniya, S. A. Sheikholeslamzadeh, H. Nasiri, and S. Emami, "Classification of breast tumors based on histopathology images using deep features and ensemble of gradient boosting methods," *Comput. Electr. Eng.*, vol. 103, Article 108382, Oct. 2022, doi: 10.1016/J.COMPELECENG.2022.108382.
- [21] "Comprehensive cancer information - NCI," [Online]. Available: <https://www.cancer.gov/>. Accessed: Dec. 13, 2022.
- [22] A. A. Adjei, "Lung cancer worldwide," *J. Thorac. Oncol.*, vol. 14, no. 6, p. 956, Jun. 2019, doi: 10.1016/j.jtho.2019.04.001.
- [23] S. T. Krishna, R. M. Devarapalli, T. K. Sajja, and H. K. Kalluri, "Lung cancer detection based on CT scan images by using deep transfer learning," doi: 10.18280/ts.360406.
- [24] S. Gao, G. Zhang, Y. Lian, L. Yan, and H. Gao, "Exploration and analysis of the value of tumor-marker joint detection in the pathological type of lung cancer," *Cell Mol. Biol.*, vol. 66, no. 6, pp. 93-97, Sep. 2020, doi: 10.14715/CMB/2020.66.6.17.
- [25] C. M. Rudin, E. Brambilla, C. Faivre-Finn, and J. Sage, "Small-cell lung cancer," *Nat. Rev. Dis. Prim.*, vol. 7, no. 1, pp. 1-20, Jan. 2021, doi: 10.1038/s41572-020-00235-0.
- [26] D.-J. Bae, J. A. Jun, S. Chang, J. S. Park, and C.-S. Park, "Epigenetic changes in asthma: Role of DNA CpG methylation," 2020, doi: 10.4046/trd.2018.0088.
- [27] K. Kirca and S. Kutlutürkan, "The effect of progressive relaxation exercises on treatment-related symptoms and self-efficacy in patients with lung cancer receiving chemotherapy," *Compl. Ther. Clin. Pract.*, vol. 45, Article 101488, Nov. 2021, doi: 10.1016/J.CTCP.2021.101488.
- [28] "Lung cancer detection using digital image processing techniques: A review," *Mehran Univ. Res. J. Eng. Technol.*, Accessed: Jan. 7, 2023. [Online]. Available: <https://search.informit.org/doi/abs/10.3316/informit.291574439064900>.
- [29] S. Kummer, J. Waller, M. Ruparel, J. Cass, S.M. Janes, and S.L. Quaipe, "Mapping the spectrum of psychological and behavioural responses to low-dose CT lung cancer screening offered within a Lung Health Check," *Health Expect*, vol. 23, no. 2, pp. 433-441, Apr. 2020, doi: 10.1111/HEX.13030.
- [30] A. Asuntha and A. Srinivasan, "Deep learning for lung cancer detection and classification," *Multimed Tool Appl*, vol. 79, no. 11-12, pp. 7731-7762, Mar. 2020, doi: 10.1007/S11042-019-08394-3.
- [31] A. Asuntha and A. Srinivasan, "Deep learning for lung cancer detection and classification," *Multimed Tool Appl*, vol. 79, no. 11-12, pp. 7731-7762, Mar. 2020, doi: 10.1007/S11042-019-08394-3.
- [32] I. Nazir, I.U. Haq, M.M. Khan, M.B. Qureshi, H. Ullah, and S. Butt, "Efficient pre-processing and segmentation for lung cancer detection using fused CT images," *Electronics*, vol. 11, no. 1, p. 34, Dec. 2021, doi: 10.3390/ELECTRONICS11010034.

- [33] Y. Yang et al., "Identification and validation of efficacy of immunological therapy for lung cancer from histopathological images based on deep learning," *Front Genet*, vol. 12, p. 121, Feb. 2021, doi: 10.3389/FGENE.2021.642981.
- [34] R. Student and N. Gupta, "Lung cancer detection using machine learning algorithms and neural network on a conducted survey dataset lung cancer detection," *Int J Innov Sci Res Technol*, vol. 8, no. 6, 2023. [Online]. Available: www.ijisrt.com
- [35] A.K. Shaji and B. Rapheal, "Lung cancer prediction using machine learning," doi: 10.56726/IRJMETS37797.
- [36] Z. Wan, "Prediction and visualization analysis of lung cancer risk by machine learning," *Highlight Sci Eng Tech*, vol. 39, pp. 221-229, Apr. 2023, doi: 10.54097/hset.v39i.6531.
- [37] J. Al-Tawalbeh, B. Alshargawi, H. Alquran, W. Al-Azzawi, W.A. Mustafa, and A. Alkhayyat, "Classification of lung cancer by using machine learning algorithms," in *IICETA 2022 - 5th International Conference on Engineering Technology and its Applications*, 2022, pp. 528-531, doi: 10.1109/IICETA54559.2022.9888332.
- [38] Z. Zheng et al., "KD_ConvNeXt: Knowledge distillation-based image classification of lung tumor surgical specimen sections," *Front Genet*, vol. 14, 2023, doi: 10.3389/FGENE.2023.1254435.
- [39] S. Doppalapudi, R.G. Qiu, and Y. Badr, "Lung cancer survival period prediction and understanding: Deep learning approaches," *Int J Med Inf*, vol. 148, Article 104371, Apr. 2021, doi: 10.1016/J.IJMEDINF.2020.104371.
- [40] N.M. Elshennawy and D.M. Ibrahim, "Deep-pneumonia framework using deep learning models based on chest X-ray images," *Diagnostics*, vol. 10, no. 9, p. 649, Aug. 2020, doi: 10.3390/DIAGNOSTICS10090649.
- [41] K.S. Beck et al., "DeepCUBIT: Predicting lymphovascular invasion or pathological lymph node involvement of clinical T1 stage non-small cell lung cancer on chest CT scan using deep cubical nodule transfer learning algorithm," *Front Oncol*, vol. 11, Article 661244, Jul. 2021, doi: 10.3389/FONC.2021.661244.
- [42] X. Wang et al., "Dual-scale categorization based deep learning to evaluate programmed cell death ligand 1 expression in non-small cell lung cancer," *Medicine*, vol. 100, no. 20, Article E25994, May 2021, doi: 10.1097/MD.00000000000025994.
- [43] M.G. Lanjewar, K.G. Panchbhai, and P. Charanarur, "Lung cancer detection from CT scans using modified DenseNet with feature selection methods and ML classifiers," *Expert Syst Appl*, vol. 224, Aug. 2023, doi: 10.1016/J.ESWA.2023.119961.
- [44] M. Sohaib and M. Adewunmi, "Artificial intelligence based prediction on lung cancer risk factors using deep learning," *Int J Inf Commun Technol*, vol. 12, no. 2, pp. 188-194, Apr. 2023, doi: 10.11591/ijict.v12i2.pp188-194.
- [45] K. Alshamrani and H.A. Alshamrani, "Classification of chest CT lung nodules using collaborative deep learning model," *J Multidiscip Healthc*, vol. 17, p. 1459, 2024, doi: 10.2147/JMDH.S456167.
- [46] M. R. Ankoliya, "Lung cancer type classification," [Online]. Available: <https://scholarworks.lib.csusb.edu/etd>. Accessed: June 7, 2024.
- [47] H. F. Kareem, M. S. Al-Husieny, F. Y. Mohsen, E. A. Khalil, and Z. S. Hassan, "Evaluation of SVM performance in the detection of lung cancer in marked CT scan dataset," *Indonesian Journal of Electrical Engineering and Computer Science*, vol. 21, no. 3, pp. 1731-1738, Mar. 2021, doi: 10.11591/IJEECS.V21.I3.PP1731-1738.
- [48] A. Campanella et al., "Diagnosis of lung cancer based on CT scans using CNN," *IOP Conference Series: Materials Science and Engineering*, vol. 928, no. 2, Article 022035, Nov. 2020, doi: 10.1088/1757-899X/928/2/022035.



INTERNATIONAL
STANDARD
SERIAL
NUMBER
INDIA



INTERNATIONAL JOURNAL OF INNOVATIVE RESEARCH

IN SCIENCE | ENGINEERING | TECHNOLOGY

 9940 572 462  6381 907 438  ijirset@gmail.com



www.ijirset.com

Scan to save the contact details